J Biol Phys (2007) 33:61–66
DOI 10.1007/s10867-007-9042-3

RESEARCH PAPER

High-Frequency Ultrasound Assessment of Antimicrobial Photodynamic Therapy In Vitro

Ralph E. Baddour · Farhan N. Dadani · Michael C. Kolios · Stuart K. Bisland

Received: 29 November 2006 / Accepted: 13 June 2007 /
Published online: 11 July 2007

Abstract Ultrasound imaging is proving to be an important tool for medical diagnosis of dermatological disease. Backscatter spectral profiles using high-frequency ultrasound (HFUS, 10–100 MHz) are sensitive to subtle changes in eukaryotic cellular morphology and mechanical properties that are indicative of early apoptosis, the main type of cell death induced following photodynamic therapy (PDT). We performed experiments to study whether HFUS could also be used to discern changes in bacteria following PDT treatment. Pellets of planktonic *Staphylococcus aureus* were treated with different PDT protocols and subsequently interrogated with HFUS. Changes in ultrasound backscatter response were found to correlate with antimicrobial effect. Despite their small size, distinct changes in bacterial morphology that are indicative of cell damage or death are detectable by altered backscatter spectra from bacterial ensembles using HFUS. This highlights the potential for HFUS in rapidly and non-invasively assessing the structural changes related to antimicrobial response.

Keywords Antimicrobial photodynamic therapy · Cell death · High-frequency ultrasound · Ultrasound backscatter

1 Introduction

There is growing interest in the capacity for photodynamic therapy (PDT) to kill bacteria as its efficacy is independent of antibiotic sensitivity and, unlike antibiotics, acquired resistance does not appear to be a risk [1]. It is clear from published reports that the antimicrobial action of PDT is very much dependent on the photosensitizer being used and

R. E. Baddour (✉) · M. C. Kolios
Department of Medical Biophysics, University of Toronto, Toronto, Canada
e-mail: rbaddour@uhnres.utoronto.ca

F. N. Dadani · S. K. Bisland
Ontario Cancer Institute, University Health Network, Toronto, Canada

M. C. Kolios
Department of Physics, Ryerson University, Toronto, Canada

the bacterial strain being targeted for kill [2]. Since skin wounds often involve multiple strains of bacteria, it is unlikely that one would completely eradicate an infection following a single regimen of PDT. Therefore, being able to non-invasively assess the antimicrobial response to PDT, in real-time, during or immediately after treatment, could allow for better treatment planning and reduced likelihood of recurrence. High-frequency ultrasound (HFUS), a relatively new imaging modality, has recently been shown to allow assessment of cell death, including apoptosis, in eukaryotic cells treated with PDT [3]. Cell death, whether apoptosis or necrosis, involves significant structural changes. For instance, in eukaryotes, apoptotic cells typically display altered distributions of membrane phospholipids, condensed chromatin, and budding vesicles from the plasma membrane [4]. There is evidence that an apoptotic-like death process exists for bacteria when they are exposed to sub-lethal stress [5]. In this study, we evaluated whether bacterial damage or death induced by PDT can be assessed using HFUS.

2 Materials and Methods

2.1 Sample Preparation and Treatment

Staphylococcus aureus (Xen29; Xenogen, Alameda, CA, USA) was selected for this experiment due to its large role in clinical infections and the increasing prevalence of antibiotic resistant strains. *S. aureus* was inoculated in flasks containing tryptic soy broth (TSB) composed of pancreatic digest of casein (17 g/l), enzymatic digest of soybean meal (3 g/l), dextrose (2.5 g/l), sodium chloride (5 g/l) and dipotassium phosphate (2.5 g/l) dissolved in pure distilled autoclaved water (pH 7.3±0.2). Once inoculated, the flasks were incubated with agitation at 37°C under ambient air for 24 h. Values for optical density (2.5 at 620 nm) and plate count (62×10^7 cfu/ml) were measured immediately prior to treatments at the 20-h incubation mark.

Two flasks were treated with 1 mmol/l of 5-aminolevulinic acid (ALA), known to be ineffective with *S. aureus* at low doses since it induces insufficient biosynthesis of protoporphyrin IX (the actual photosensitizer) [6]. Since no significant antimicrobial response with PDT was anticipated, ALA was considered as a suitable control. Another two flasks were treated with 0.1 mmol/l of methylene blue (MB), a photosensitizer shown to be effective at killing *S. aureus* during PDT [7, 8]. After the prescribed drug incubation periods (4 h for ALA, 1 h for MB), the cells were centrifuged twice (1,000×*g* for 5 min, 4,500×*g* for 5 min) to produce dense pellets (approximately 4 mm in height) in flat-bottomed vials. For ALA-PDT, one ALA-treated pellet was drained of its supernatant and irradiated with a custom-built 635 nm (±5 nm), 300 mW light-emitting diode laser (Laboratory of Applied Biophotonics, University Health Network, Toronto, ON, Canada), with the beam collimated onto the whole pellet surface to achieve an effective fluence of 20 J/cm^2. The MB-PDT was performed in the same fashion on one of the MB-treated pellets, but with a 670 nm (±5 nm) laser (same manufacturer). Both PDT regimens were performed with equivalent irradiation periods of 1,000 s.

2.2 Ultrasound Data Acquisition

Immediately after treatments, all four pellets, submerged in TSB and kept in the dark, were insonified from above with broadband 20 and 40 MHz ultrasound pulses using two focused transducers (with corresponding resonant frequencies) and a VS40b ultrasound device

(VisualSonics, Toronto, ON, Canada). This device allows for the selection of a region of interest (ROI) from the brightness-mode (B-mode) images and stores the associated raw, unprocessed A-scan lines from that region. For each pellet, a 0.5 mm (in depth) ROI was selected below the pellet surface, centred on the transducer's focal depth. The average backscatter power spectrum was calculated by averaging the squared magnitude of the Fourier transforms of each of the 350 independent A-scans acquired. To eliminate any system or transducer-specific effects, all of the spectra were normalized to the power spectrum of the echo from a calibration target, a flat, polished SiO_2 crystal (Edmund Optics, Barrington, NJ, USA; part 43424).

2.3 Transmission Electron Microscopy

Although numerous techniques exist for cell sizing, electron microscopy was used in this study since it additionally provides structural information. In parallel with the ultrasound measurements, duplicate *S. aureus* pellets were prepared. After treatments, the pellets were resuspended in a 2% agarose solution, fixed with glutaraldehyde, followed by an en bloc fixation with 2% uranyl acetate, fixed in osmium tetroxide, dehydrated by alcohol gradient, and then infiltrated with Spurr's resin. Transmission electron micrographs (TEM) of these samples were acquired with a TEM-7000 instrument (Hitachi High Technologies America, Pleasanton, CA, USA).

2.4 Cell Viability Assay

The same sample preparation and treatment procedure performed to produce the samples destined for ultrasound data acquisition was repeated for an additional set of samples to measure cell viability. Standard methodologies for determining the relative bacterial cell kill were used [9]. Briefly, serially diluted preparations of each sample (ALA, ALA + light, MB, MB + light) were prepared and plated in triplicate onto Luria-Bertani agar (BD Diagnostics, Sparks, MD, USA). Plates were incubated at 37°C for 24 h prior to counting the number of colonies. Cell kill was calculated as the ratio between the measured mean cfu/ml values from the PDT-treated and drug-only control samples.

3 Results

Ultrasound B-mode imaging and backscatter measurements were performed on the four different pellets of *S. aureus*: two photosensitizer-only control samples (treated with ALA or MB) and two PDT samples (ALA + 630 nm light, MB + 670 nm light). The results of the ALA test are shown in Fig. 1 and MB test results are presented in Fig. 2. The normalized backscattered power spectra are expressed in decibels relative (dBr) to the backscatter intensity from the SiO_2 calibration target. The backscatter spectra are shown for the frequency ranges corresponding to the 6 dB bandwidths of each transducer employed (approximately 10–30 MHz for the 20 MHz transducer and 20–50 MHz for the 40 MHz transducer).

The ALA-PDT treatment was found to yield a 0.12 log cell kill. For the MB-PDT protocol, 3.5 log cell kill was achieved. Representative TEM images of individual bacteria from each treatment group are presented in Figs. 1 and 2 (inset). Because the samples were fixed immediately after PDT treatment, only early changes associated with death were observed in the MB-PDT sample (Fig. 2b). Digital image analysis was performed on 20

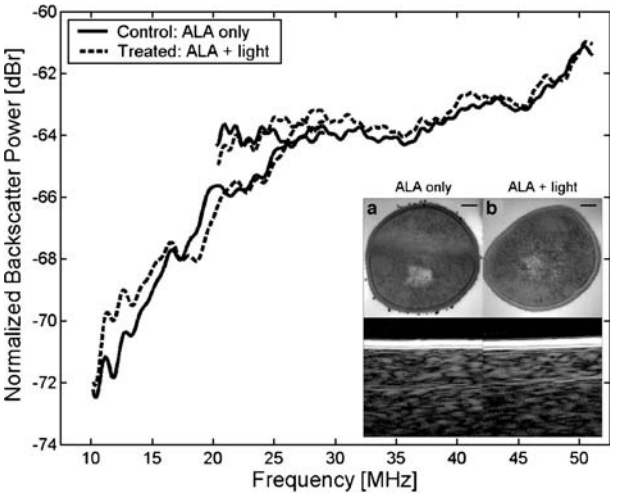

Fig. 1 Ultrasound spectral data acquired using two wideband transducers (resonant frequencies: 20, 40 MHz) from pellets of *S. aureus* treated with 5-aminolevulinic acid (1 mmol/l), unexposed to light (control; *solid curves*) and irradiated with 20 J/cm^2 of 635 nm light (treated; *dashed curves*). Transmission electron micrographs of representative **a** control and **b** treated bacteria are presented (*inset*, ×150,000 magnification, *scale bars* represent 100 nm), along with typical ultrasound B-mode images from the top of each respective pellet acquired using the 20 MHz transducer (*bottom inset*, 1.5 mm^2 region shown)

randomly selected, in-focus cells from each TEM data set. Using a manual outlining technique, cells from the two control samples and the ALA-PDT sample were found to have the same area (0.37±0.01 μm^2). Cells from the MB-PDT group, however, were over 16% larger (0.43±0.01 μm^2), mainly due to an increase in the apparent thickness of the peptidoglycan layer (as seen in Fig. 2b).

4 Discussion

As expected, the chosen ALA-PDT protocol had negligible antimicrobial effect and *S. aureus* appeared structurally intact in TEM. As shown in Fig. 1, ultrasound backscatter response was similarly unaffected. By contrast, MB-PDT-treated pellets revealed considerable cell kill and nearly a two-fold increase in ultrasound backscattering across the 10–50 MHz band. One possible contribution to this effect is the likely mechanical

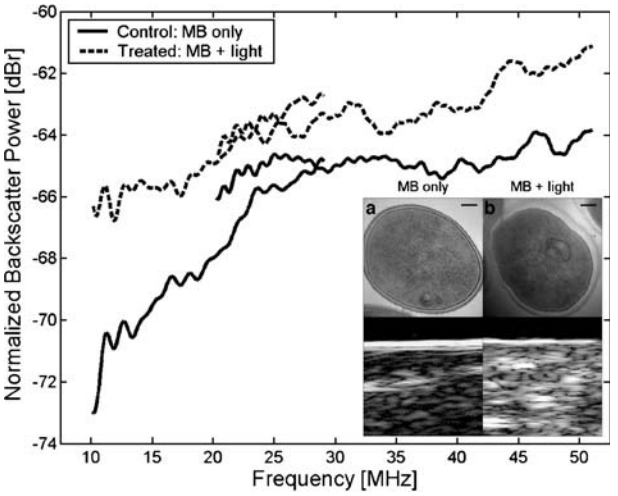

Fig. 2 Ultrasound spectral data acquired using two wideband transducers (resonant frequencies: 20, 40 MHz) from pellets of *S. aureus* treated with methylene blue (0.1 mmol/l), unexposed to light (control; *solid curves*) and irradiated with 20 J/cm^2 of 670 nm light (treated; *dashed curves*). Transmission electron micrographs of representative **a** control and **b** treated bacteria are presented (*inset*, ×150,000 magnification, *scale bars* represent 100 nm), along with typical ultrasound B-mode images from the top of each respective pellet acquired using the 20 MHz transducer (*bottom inset*, 1.5 mm^2 region shown)

property changes during the peptidoglycan layer destruction process (initial thickening followed by disintegration). However, the increase in overall cell size probably has a more important role. One would expect Rayleigh scattering [10] for scatterers as small as bacteria (<1 μm), relative to the much larger wavelengths of incident sound (in TSB: 77 μm at 20 MHz, 39 μm at 40 MHz). In the Rayleigh regime, when scatterers are much smaller than the sound wavelength, backscatter is proportional to the sixth power of the diameter.

The normalized backscattered spectra presented in Figs. 1 and 2 were approximately continuous across the two different transducers. A trend of reducing slope with increasing frequency is evident. This "corner" may indicate that the band of frequencies investigated represents a transition zone in the scattering response of *S. aureus*. However, even the steeper slopes of the 20 MHz transducer-acquired segments (for both plots in Fig. 1 and the control in Fig. 2) are only approximately 0.4 dB/MHz (assuming a linear fit to the data). This is much lower than the value of 1.2 dB/MHz needed to meet the fourth-power frequency dependence predicted for Rayleigh scattering [10]. Smaller spectral slopes indicate a larger effective scatterer size [11]. It is possible that, when in pellet, some bacterial agglomeration occurs. After MB-PDT, the slope of the 20 MHz region of the backscatter response reduces to 0.18 dB/MHz. This could indicate the presence of larger aggregates.

The sensitivity and specificity of HFUS at correctly detecting early changes induced in *S. aureus* by MB-PDT indicates that this technique might have the potential to be used in a pre-clinical setting for evaluating different irradiation protocols and photosensitizers for antimicrobial PDT. This would be a useful assay since it is non-invasive, real-time, could be performed in parallel to irradiation, and does not require the addition of any contrast agents or stains. Although large bacterial populations are required to generate samples thick enough for backscatter spectral analysis, the use of even higher frequency sound, to improve the imaging resolution, could alleviate this requirement. It will also be necessary to consider a suite of both Gram-positive and -negative strains in future studies to attempt to decipher general backscatter patterns seen across all bacterial species.

Acknowledgements R.E.B. and F.N.D. contributed equally to this work. The authors acknowledge G. Nathanael for experimental assistance. The authors also thank B. Calvieri and S. Doyle for technical assistance with TEM. Financial support for this work was provided by the Canadian Institutes of Health Research and the Natural Sciences and Engineering Research Council of Canada. The ultrasound imaging device was purchased with funds from the Canadian Foundation for Innovation, the Ontario Innovation Trust, and Ryerson University.

References

1. Maisch, T., Szeimies, R.M., Jori, G., et al.: Antibacterial photodynamic therapy in dermatology. Photochem. Photobiol. Sci. **3**, 907–917 (2004)
2. Demidova, T.N., Hamblin, M.R.: Photodynamic therapy targeted to pathogens. Int. J. Immunopathol. Pharmacol. **17**, 245–254 (2004)
3. Czarnota, G.J., Kolios, M.C., Abraham, J., et al.: Ultrasound imaging of apoptosis: High-resolution non-invasive monitoring of programmed cell death in vitro, in situ and in vivo. Brit. J. Cancer **81**, 520–527 (1999)
4. Hacker, G.: The morphology of apoptosis. Cell Tissue Res. **301**, 5–17 (2000)
5. Aldsworth, T.G., Sharman, R.L., Dodd, C.E.R.: Bacterial suicide through stress. Cell. Mol. Life Sci. **56**, 378–383 (1999)

6. Nitzan, Y., Salmon-Divon, M., Shporen, E., et al.: ALA induced photodynamic effects on Gram positive and negative bacteria. Photochem. Photobiol. Sci. **3**, 430–435 (2004)
7. Hamblin, M.R., Hasan, T.: Photodynamic therapy: A new antimicrobial approach to infectious disease? Photochem. Photobiol. Sci. **3**, 436–450 (2004)
8. Bisland, S.K., Chien, C., Wilson, B.C., et al.: Pre-clinical in vitro and in vivo studies to examine the potential use of photodynamic therapy in the treatment of osteomyelitis. Photochem. Photobiol. Sci. **5**, 31–38 (2006)
9. Liu, X., Wang, S., Sendi, L., et al.: High-throughput imaging of bacterial colonies grown on filter plates with application to serum bactericidal assays. J. Immunol. Methods **292**, 187–193 (2004)
10. Strutt, J.W.: Investigation of the disturbance produced by a spherical obstacle on the waves of sound. Proc. London Math. Soc. **4**, 233–283 (1872)
11. Lizzi, F.L., Astor, M., Liu, T., et al.: Ultrasonic spectrum analysis for tissue assays and therapy evaluation. Int. J. Imaging Syst. Technol. **8**, 3–10 (1997)